Journal of Information Hiding and Multimedia Signal Processing ©2016 ISSN 2073-4212
Ubiquitous International Volume **7**, Number **5**, September **2016**

A Novel Method for Road Centerline Extraction from High Spatial Resolution Satellite Images

Rui Xu[1,2,3]

[1] Key Lab of Spatial Data Mining & Information Sharing of Ministry of Education,
Spatial Information Research Center of Fujian Province
Fuzhou University
No.523, Gongye Road, Fuzhou, 350002, China

[2] College of Information Science and Engineering
Fujian University of Technology
No.3, Xueyuan Road, University Town, Fuzhou, 350108, China

[3] Fujian Provincial Key Laboratory of Big Data Mining and Applications
Fujian University of Technology
No.3, Xueyuan Road, University Town, Fuzhou, 350108, China
dr.xurui@126.com

Received May, 2016; revised July, 2016

Abstract. *An integrated method for road centerline extraction has been proposed in this paper which consists of four main steps. First, the Graph Cut algorithm using proposed similarity function is employed to segment the image, and the segmented image is thresholded to initial binary skeleton. Second, the road skeleton is refined by using a series of morphology operations and shape features. Third, the curvilinear feature of road skeleton is detected by a set of multiple filtering detectors. Finally,a regression method is performed to extract smooth and accurate road centerlines. Validation tests show that the proposed method is able to achieve a comparatively good performance in road centerline extraction from high spatial resolution satellite images.*
Keywords: High resolution image, Road centerline extraction, Graph cut, Curvilinear structure, Regression method.

1. **Introduction.** The advent of modern sensors in recent years makes it possible to utilize high spatial resolution satellite (HSRS) images which can provide rich spatial and spectral information. The extracted road network from HSRS images has many important and diverse applications, such as geographic information system (GIS) database update, urban mapping and planning, navigation, change detection, image registration, etc. A number of algorithms in this area have been proposed over the past decades. Mena [1], Mena and Malpica [2] and Das et al. [3] provided an overview and categorization of the related work. Generally speaking, road extraction commonly includes two main fields: road objects detection and centerline extraction.

Road objects detection is the most important processing which aims to detect road candidate from satellite images. We briefly highlight the representative work in the following. In [4], Song and Civco proposed a three-step-based method to detect road objects. In their method, a support vector machine (SVM) was used to classify the input image into road and non-road groups. Similarly, Shi et al. [5] combined spectral-spatial and shape features to extract urban main road. In the first step, they segmented the imagery into

the road class and the non-road class using spectral-spatial classification. Then remotely sensed imagery was homogenized by using local Geary 's C. As a final step, the road class was refined by using shape features. The experimental results indicated that the method they proposed could achieve a comparatively good performance in urban main road extraction. Poullis and You [6] presented an object-based system for automatic road detection, which includes methods like Gabor filtering, tensor voting and orientation-based segmentation.Object-oriented approach can achieve high accuracy in most cases. However, with the increase in complexity of the road network, Object-oriented approach can't solve the road extraction problem completely. Therefore, knowledge-based approach incorporating both low-level image-based recognition techniques as well as higher-level knowledge is widely used. Sun and Messinger [7] proposed a knowledge-based automated road network extraction algorithm based on curvilinear detector and knowledge-based system. Hu et al. [8] employed spoke wheel operator and toe-finding algorithms to track road footprints, followed by refinement by road tree pruning. Several other approaches have been developed from different viewpoints to deal with the detection of road objects, including mathematical morphology [9],edge-based approaches [10],snakes [11],template matching [12],active testing [13], etc. Though the above-mentioned approach strive to detect road objects with some degree of satisfaction, the complete automation of road objects detection remains a hard problem which has not been solved with a reasonable degree of success.

Centerline extraction from road skeleton is another set of important processing. The concept of centerline was introduced by Blum [14]. There are a few kinds of centerline extraction methods: 1) Thinning algorithm. Topology thinning algorithm [15], also called onion peeling, is a traditional thinning method. In its realization process, objects are peeled level by level and the points are deleted while the topology of model remains unchanged. This method can keep the whole connectedness of the model, but it's an iteration process requiring a huge amount of computation. It often performs well on 3D skeletons, and can also be used for 2D road skeletons. Morphological thinning algorithm [4] is another traditional thinning method which is always used to extract road centerline. 2) Shortest path finding such as geodesic method[16], is an algorithm aiming at finding the shortest path from a start point to an end point. Its advantage is low computation and high speed. The disadvantage is that the path is easily near to the inner wall, which means that the centerline is not at the center position. 3) Level set marching[17] is to embed the moving boundary as a zero level-set into a higher level-set function and extract the centerline by computing the evolution curve. It is very robust but the energy function of the fast marching method is difficult to get. 4) Regression methods change the road centerline extraction issues into regression issues. It can perform well in extracting road centerline. Miao et al. [18]successfully and effectively extracted road centerlines from the categorized images by regression methods.

Fruitful achievements have been made by previous researchers; however, there are still a number of challenges in road detection from an image. (1) Due to the complex spatial arrangement and spectral heterogeneity even within the same class, the accurate detection of the road objects is a problem not satisfactorily solved by existing approaches. (2) The accuracy of current centerline extraction methods is far from satisfaction. The results may produce many spurs or can't cover the ground truth centerlines completely. To overcome the drawbacks, this paper tries to go further in road centerline extraction approach from HSRS images. Firstly, we design an appropriate similarity function for graph cut algorithm to improve the robustness and accuracy of segmentation. Secondly, we design a set of suitably post processing stages to refine the skeleton of road, and centerlines are extracted from the refined skeleton by integrating a set of curvilinear feature detectors

and a regression method. Experiments show that the proposed method is able to achieve a comparatively good performance in road centerline extraction.

The remainder of this paper is organized as follows. The new approach is presented in Section 2. Experimental results are presented and discussed in Section 3. Conclusions are provided in Section 4.

2. **Methodology.** The proposed method is presented in this section. The organization of this method is shown in Fig.1. The details of each step are introduced as follows.

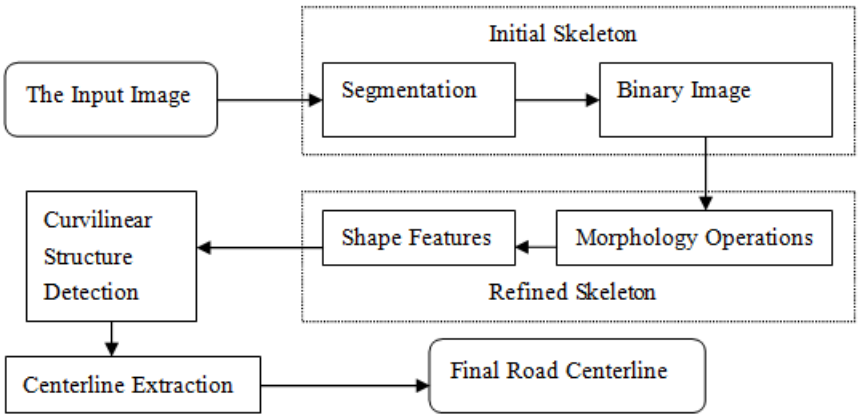

FIGURE 1. Flowchart of proposed method.

2.1. Unsupervised Parametric Graph Cut Segmentation.

2.1.1. *Parameter Kernel Graph Cut.* Here, the parametric kernel graph cut[19] which is an unsupervised method is used to segment HSRS images. Let $I : p \in \Omega \subset R^2 \to I_p = I(p) \in I$ be an image function from a positional array Ω to a space I of photometric variables such as intensity, disparities, color or texture vectors. Segmenting I into N_{reg} regions consists of finding a partition $\{R_l\}_{l=1}^{N_{reg}}$ of the discrete image domain so that each region is homogeneous with respect to some image characteristics.

Let $\varphi(.)$ be a nonlinear mapping from the observation space I to a higher (possibly infinite) dimensional feature mapped space J. A given labeling assigns each pixel a label and, consequently, divides the image domain into multiple regions. Each region is characterized by one label: $R_l = \{p \in \Omega | \lambda(p) = l\}, 1 \leq l \leq N_{reg}$.Solving image segmentation in a kernel-induced space with graph cut consists of finding the labeling which minimizes.

$$F_k(\{\mu_l\}, \lambda) = \sum_{l \in L} \sum_{p \in R_l} (\varphi(\mu_l) - \varphi(I_p))^2 + \alpha \sum_{\{p,q\} \in N} r(\lambda(p), \lambda(q)) \tag{1}$$

F_k measures kernel-induced non Euclidean distances between the observations and the regions parameters μ_l for $1 \leq l \leq N_{reg}$. In machine learning, the kernel trick consists of using a linear classifier to solve a nonlinear problem by mapping the original nonlinear data into a higher dimensional space. We can use a kernel function,$K(y, z)$, verifying

$$K(y, z) = \varphi(y)^T \cdot \varphi(z), \forall (y, z) \in I^2 \tag{2}$$

where "." is the dot product in the feature space. Using this kernel function, the objective functional minimization is carried out by iterations of two consecutive steps: a) minimization with respect to the image segmentation by graph cut and b) minimization

with respect to the regions parameters via fixed point computation. Salah et al. [19] provided the details of each step about this parametric kernel graph cut.

2.1.2. *Construction of Similarity Function.* Similarity function is essential for the results of graph cut methods. The commonly used similarity function is Gauss function. The Gauss function g^0 is defined as

$$g^0 = \exp\left(-\frac{\|v_i - v_j\|^2}{\sigma^2}\right) \tag{3}$$

where $\|*\|$ is the Euclidean distance,v_i is the value of pixel i, σ is the scale factor which usually denotes global variance distance. Due to the complex spatial arrangement and spectral heterogeneity even within the same class, similarity function with single factor can't achieve satisfactory segment results. Therefore, this paper constructs a novel similarity function by integrating color similarity index, angle distribution index, location index, and edge gradient magnitude index.

(1) Color Similarity Index

Here HSV color space is used in which Hue is used to distinguish colors; Saturation is the percentage of white light added to a pure color and Value refers to the perceived light intensity. In this paper, three-component vector of HSV is converted to one-dimensional vector I and $I = 9H + 3S + V$. Color Similarity Index g_I is defined as

$$g_I(i,j) = \exp\left(-\frac{\|I_i - I_j\|^2}{\sigma_I^2}\right) \tag{4}$$

(2) Angle Distribution Index

In pixel-i-centered statistics window, there are M different edges with M different angles which are denoted as $\theta_1, ..., \theta_M$. A_I is defined as $A_i = \sum_{k=1}^{M} \theta_k / M$. The Angle Distribution Index g_A is computed as

$$g_A(i,j) = \exp\left(-\frac{\|A_i - A_j\|^2}{\sigma_A^2}\right) \tag{5}$$

(3) Location Index

The Location Index g_L is defined as

$$g_L(i,j) = \exp\left(-\frac{\|L_i - L_j\|^2}{\sigma_L^2}\right) \tag{6}$$

where L_i and L_j are the position of the pixel i and the pixel j respectively. When the value of $\|L_i - L_j\|$ is getting smaller, the adjacent pixel i and pixel j in the spatial position are getting closer, which means they are more likely to belong to the same object.When the value of $\|L_i - L_j\|$ is greater than the threshold, the influence of the Location Index can be neglected.

$$g_L(i,j) = \begin{cases} 0 & \|L_i - L_j\| > t \\ g_L(i,j) & \|L_i - L_j\| \le t \end{cases} \tag{7}$$

(4) Edge Gradient Magnitude Index

The Edge Gradient Magnitude Index g_E is computed as

$$g_E(i,j) = \exp\left(-\left(\frac{|\max(\text{edge}(x))|^2}{\sigma_E^2}\right)\right) \tag{8}$$

where $line(i,j)$ is the line between pixel i and the pixel j, $x \in line(i,j)$, $edge(x)$ donates the edge gradient magnitude of intersection point x of edge and $line(i,j)$.

Taking into account the above-mentioned four indexes and $\omega 1, \omega 2, \omega 3, \omega 4$ as the weight of each index, we define similarity function for pixel i and pixel j as

$$s(i,j) = \exp\left(-\frac{\|I_i - I_j\|^2}{\omega_1\sigma_I^2} - \frac{\|A_i - A_j\|^2}{\omega_2\sigma_A^2}\right) + \exp\left(-\frac{\|L_i - L_j\|^2}{\omega_3\sigma_L^2} - \frac{|\max(\text{edge}(x))|^2}{\omega_4\sigma_E^2}\right) \tag{9}$$

2.2. **Road Skeleton Generation.** Road skeleton is generated on the basis of the segmented images which involves the following steps. First, binarize all the possible road pixels from the segmented image. This step does not need to be very precise but it is desirable to include as many candidate road-like pixels as possible. Second, extract the morphological skeleton by using a series of morphology operations such as corrosion and open operation. Then road-like candidates are extracted. Third, improve the accuracy of road skeleton by using shape features. As remotely sensed imagery exhibits complex spectral character, misidentified roads still exist. Hence, road shape features can be used to filter false segments. These features can be measured by Area, Compactness, Slenderness and Length-width ratio, which are introduced as follows.

(1) Area refers to the number of pixels included in the region. Segments with small area values can be viewed as non-road class and be removed.

(2) Compactness is defined as $4 \cdot Pi \cdot A/P^2$, where P is perimeter of region and A is area of region. Compactness is in the range of (0, 1].

(3) Slenderness is defined as $2 \cdot A/L$, where L is the regional center line length.

(4) Length-width ratio is the aspect ratio of the minimum enclosing rectangle.

2.3. **Curvilinear Structure Detection.** By previous steps, the refined road skeleton is produced. But, the produced skeleton contains a few irregular shapes. In order to extract correct and smooth road centerlines, the curvilinear feature of road skeleton should be detected and enhanced. In this paper, we follow the method of Costas Panagiotakis et al. [20]. A set of multiple filtering detectors with different widths and directions form the polynomial filter. The one dimension polynomial filter is defined as

$$F(x) = \begin{cases} 1 - \left(\frac{x}{w}\right)^2, |x| < w \\ c_p.\left(\left(\frac{x}{w} - 2\right)^2 - 1\right), w \le |x| < r.w \\ 0, |x| \ge r.w \end{cases} \tag{10}$$

where x is one of the pixels in the filter bank, the parameter w is representative of the road width. The parameter r which should be greater than one, is expressed as the relaxed space to correlate with road boundaries. The constant c_p is a positive number, estimated by the constraint that the 2-D filter is zero mean.

Let $F(a,w)$ be a zero mean polynomial filter (see Fig.2) of orientation angle a and width w. The convolution of I_d with the $F(a,w)$ for different angles a and widths w is computed, yielding the images $I_f(a,w)$

$$I_f(a,w) = |I_d * F(a,w)| \tag{11}$$

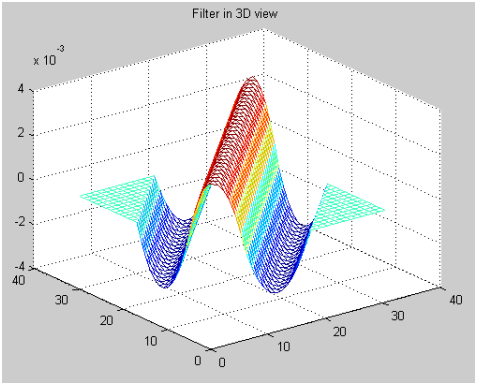

FIGURE 2. Three-dimensional (3-D) view of Polynomial filter.

Image $I_f(a, w)$ hosts an enhancement of the curvilinear structures of orientation a and width w. Eighteen different angles and three different widths were employed. The resulting image I_m is provided by getting the maximum of the corresponding pixel values of images $I_f(a, w)$

$$I_m = \max_{a,w} I_f(a, w) \tag{12}$$

In the resulting image, the maximum-response score map can be obtained. The curvilinear structures under any orientation and width are enhanced. As a high response score indicates a higher possibility for the road structure, road skeleton is well identified and smoothened.

2.4. **Centerline Extraction.** The mainstream centerline extraction methods include thinning algorithm and geodesic method, but both methods have their drawbacks: the thinning algorithm produces many spurs; and the results of the geodesic method can't cover ground truth centerline completely. Fig.3 shows examples of these two methods.

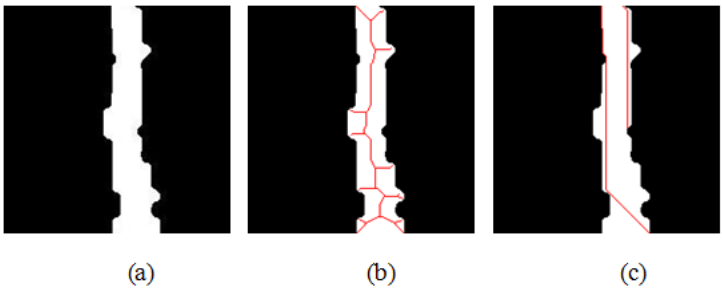

FIGURE 3. (a) Refined road skeleton. (b) Result of thinning algorithm. (c) Result of geodesic method.

Road centerline extraction from the road skeleton can be approximately equivalent to determine the quantitative relationship between x and y directions from the discrete points. The quantitative relationship can be determined on the x and y directions by regression methods. Miao et al. [18] have shown that regression methods are good at extracting centerlines from road skeleton.

Multivariate adaptive regression splines (MARS) is a nonlinear and nonparametric regression technique which was first proposed by Friedman [21]. Because it makes no

assumption about the underlying functional relationship between the dependent and prediction variables, MARS has been increasingly used in recent years in road centerline extraction.

MARS builds models from two sided truncated functions of the predictors (x) of the form:

$$(x-t)_+ = \left\{ \begin{array}{cc} x-t & x>t \\ 0 & otherwise \end{array} \right\} \tag{13}$$

These serve as basis functions for linear or nonlinear expansion that approximates some true underlying function $f(x)$. The MARS model for a dependent (outcome) variable y, and M terms, can be summarized in the following

$$y = f(x) = \beta_0 + \sum_{m-1}^{M} \beta_m H_{km}(x_{v(km)}) \tag{14}$$

where the summation is over the M terms in the model, β_0 and β_m are parameters of the model (along with the knots t for each basis function, which are also estimated from the data). Function H is defined as

$$H_{km}(x_{v(km)}) = \prod_{k=1}^{K} h_{km} \tag{15}$$

where $x_{v(km)}$ is the predictor in the $k'th$ of the $m'th$ product.

A measure of the goodness of fit is generalized cross-validation (GCV) error which is written by

$$GCV = \frac{\sum_{i=1}^{N} \left(y_i - f\left(x_i\right)\right)^2}{\left(1-\frac{C}{N}\right)^2} \quad with \quad C = 1 + cd \tag{16}$$

where N is the number of cases in the data set, d is the effective degrees of freedom, which is equal to the number of independent basis functions. The quantity c is the penalty for adding a basis function.

It is worth mentioning that extracting centerline by MARS directly from the road skeleton can not get satisfactory results. The curvilinear structures of road skeleton need to be enhanced first. Besides, MARS can't solve the issues of road network with junctions. Thus, road network should be dismantled first by utilizing road intersections, and after extracting the centerlines, junctions should be united to form road network.

3. **Experimental Study.**

In this section, several experiments are described to evaluate the performance of the proposed method which is also compared with other methods to show it's advantages and limitations.

3.1. **Experiment.**

In the first experiment, the study area is a part of Beijin City image which was recorded by the Worldview-II optical sensor. The study area has a spatial dimension of 400*400 pixels. The spatial resolution is 0.5m per pixel. Fig.4(a) shows the study area of experiment 1. The Graph Cut algorithm using our designed similarity function is firstly applied to segment the study area, with the result shown in Fig.4(b). Then the segmented image is thresholded to the binary image, with the result shown in Fig.4(c). Next the morphological skeleton is extracted using a series of morphology operations such as corrosion and open operation, with the result shown in Fig. 4(d). The

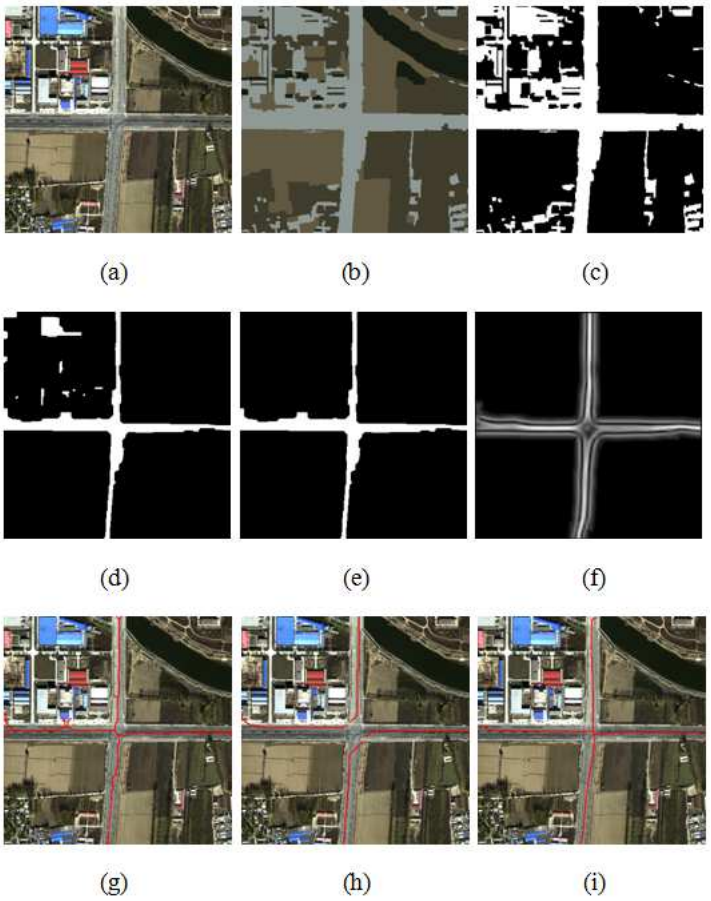

FIGURE 4. (a) Original image. (b) Result of Graph Cut using proposed similarity function.(c) Result of binarization. (d) Result of morphology operation. (e) Result of filtering by shape feature. (f) Result of the curvilinear detectors. (g) Result of the thinning method shown in red. (h) Result of the geodesic method shown in red. and (i) Result of the proposed method shown in red.

morphological skeleton is close to ground truth data, but still exists false road segments, so we apply shape feature to remove false road segments and refine the skeleton. The refined skeleton is shown in Fig. 4(e). In order to extract accurate and smooth road centerline, the curvilinear feature of road skeleton is enhanced, with the result shown in Fig.4(f). Finally, road centerlines are extracted from the curvilinear structures by MARS method, with the result shown in Fig.4(i). Fig.4(g) shows the road centerline extraction result produced by the thinning method. Fig.4(h) shows the result of the geodesic method. Compared with the results of the thinning and the geodesic methods, this proposed method can extract smooth and correct road centerlines.

In the second experiment, another satellite image was picked up to test the proposed method. The test image was recorded at Fuzhou City by QuickBird. It is shown in Fig.5(a), which has a spatial size of 400*400 pixels. The spatial resolution of this image is 2.44m per pixel. At this resolution, small roads are unclear; Hence, only main roads are able to be extracted. The steps of this experiment are the same as the previous one. Fig.5(b) shows the segmentation results of our Graph Cut algorithm. It is shown that this algorithm using proposed similarity function can produce satisfactory result, but error distinction still exists.The second step is to binary the segmented image and the result is

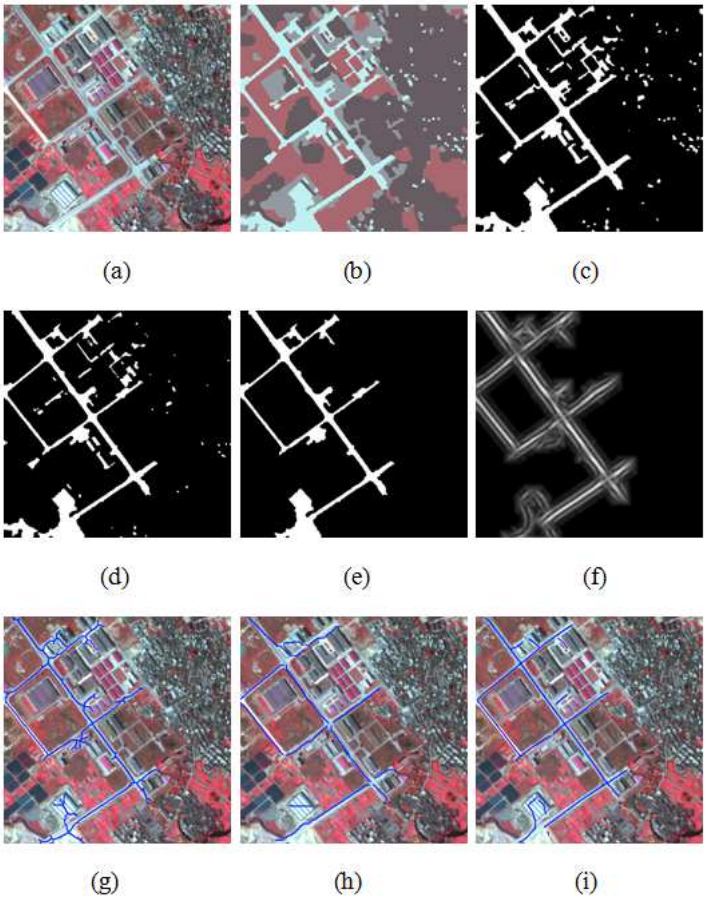

FIGURE 5. (a) Original image. (b) Result of Graph Cut using proposed similarity function.(c) Result of binarization. (d) Result of morphology operation. (e) Result of filtering by shape feature. (f) Result of the curvilinear detectors. (g) Result of the thinning method shown in blue. (h) Result of the geodesic method shown in blue. and (i) Results of the proposed method shown in blue.

given in Fig.5(c). Then the Skeleton of the road is refined by the method of morphology and the road shape feature, Fig.5(e) shows the final Skeleton of the road. Next, the curvilinear feature of road skeleton is also enhanced, with the result shown in Fig.5(f). In the final step, the MARS algorithm is performed to extract the road centerlines, the superposition result of the original image and the extracted road centerlines is given in Fig.5(i). Fig.5(g)-(h) show the results of the thinning method and the geodesic method respectively. It can be seen from this experiment that the proposed method still shows good performance, even when the road skeleton is complicated.

In the third experiment, an image with a spatial size of 602*865 pixels, downloaded from [22], was used to test the proposed methods performance. The test image is shown in Fig. 6(a). The steps of this experiment are the same as the previous two, with the results shown in Fig.6 (b-f). It can be seen clearly from Fig. 6(g) and Fig. 6(h) that neither the thinning method nor the geodesic method can extract smooth and accurate road centerline. Compared with these two methods, the proposed method is more suitable for road centerline extraction, with the results shown in Fig.6(i).

3.2. **Analysis of the experiment.** The results of the three centerline extraction methods show that the proposed method and the geodesic method provided smoother results

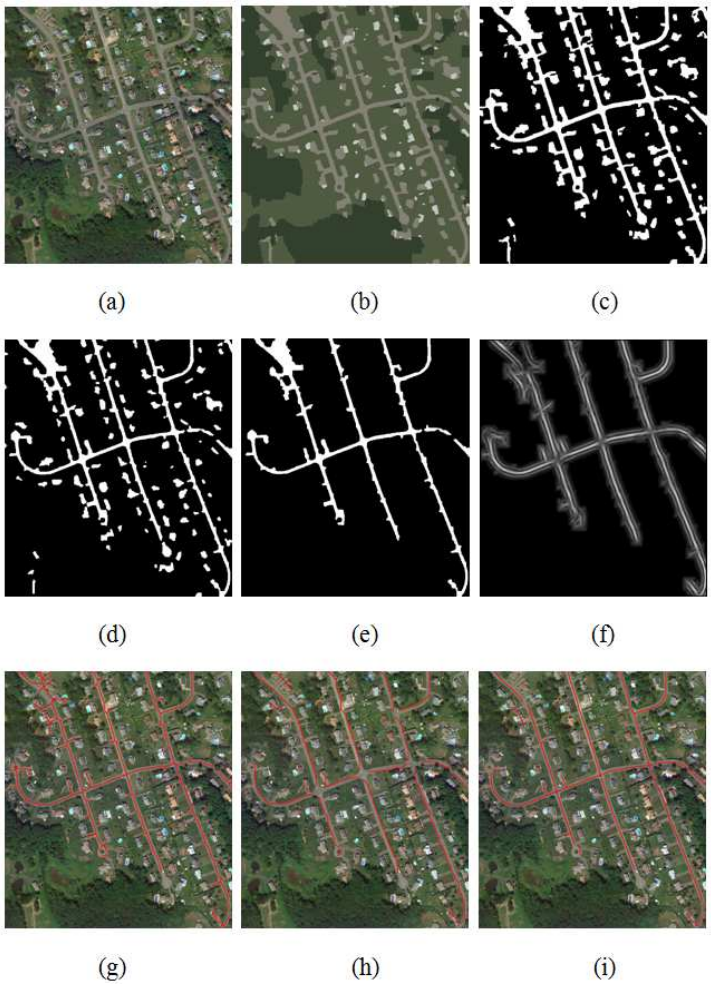

FIGURE 6. (a) Original image. (b) Result of Graph Cut using proposed similarity function. (c) Result of binarization. (d) Result of morphology operation. (e) Result of filtering by shape feature. (f) Result of the curvilinear detectors. (g) Result of the thinning method shown in red. (h) Result of the geodesic method shown in red. and (i) Result of the proposed method shown in red.

than the thinning algorithm. The thinning algorithm method produced many undesired spurs and branches, which reduced the smoothness of the road centerline. Although the geodesic method extracted a smooth result, the centerline is not at the center position.

To quantify the performance of the proposed method, three accuracy measures [23] are used to evaluate it. These measures are: 1) $completeness = TP/(TP + FN)$; 2) $correctness = TP/(TP + FP)$; and 3) $quality = TP/(TP + FP + FN)$. Here Q_1, Q_2 and ,Q_3 represent completeness, correctness, and quality, respectively. The variables TP, FN, and FP denote true positive, false negative, and false positive, respectively.

According to the results given in Table 1, it can be concluded that the proposed method provides a practical solution for accurate road centerline extraction from HSRS images with comparatively high efficiency.

4. **Conclusions.** This paper has proposed an advanced framework for road centerline extraction from HSRS images. An effective graph cut algorithm is firstly employed to

TABLE 1. Quantitative evaluation of different centreline extraction methods

Method	Experiment 1			Experiment 2			Experiment 3		
	$Q_1(\%)$	$Q_2(\%)$	$Q_3(\%)$	$Q_1(\%)$	$Q_2(\%)$	$Q_3(\%)$	$Q_1(\%)$	$Q_2(\%)$	$Q_3(\%)$
Thinning	91.18	92.08	84.55	87.25	77.39	69.53	86.27	85.45	75.21
Geodesic	87.25	89.00	78.76	78.43	86.96	70.18	71.57	90.12	66.36
Porposed	93.14	95.96	89.62	90.20	89.32	81.42	94.12	93.20	88.07

segment the HSRS image. Next, morphological method and road shape feature are designed to refine the road skeleton. Once road skeleton is extracted, a set of multiple filtering detectors are applied to enhance the curvilinear structures of the road skeleton. Finally, the MARS algorithm based on curvilinear structures is used to extract reliable road centerline. The experimental results show that the proposed method provides a more smooth and accurate extraction of road centerline than the commonly used thinning or the geodesic method.

Acknowledgment. This work is supported by the key project of science and technology of Fujian province (2014H6006), the project of science and technology of Fujian province (2016H0001), and the project of Fuzhou Municipal Science and Technology Bureau (2015-G-53).

REFERENCES

[1] J. B. Mena, State of the art on automatic road extraction for GIS update: A novel classification, *Pattern Recognition Letters*, vol.24, no.16, pp.3037–3058, 2003.

[2] J. B. Mena and J. A. Malpica, An automatic method for road extraction in rural and semi-urban areas starting from high resolution satellite imagery, *Pattern Recognition Letters*, vol. 26, no. 9, pp. 1201–1220, 2005.

[3] S. Das, T. T. Mirnalinee, and K. Varghese, Use of Salient Features for the Design of a Multistage Framework to Extract Roads From High-Resolution Multispectral Satellite Images, *IEEE Transactions on Geoscience and Remote Sensing* , vol.49, no.10, pp.3906–3931, 2011.

[4] M. Song and D. Civco, Road Extraction Using SVM and Image Segmentation, *Engineering and Remote Sensing* , vol.70, no.12, pp.1365–1372, 2004.

[5] W. Z. Shi, Z. L. Miao, Q. Wang, and H. Zhang, Spectral-spatial classification and shape features for urban road centerline extraction. *IEEE Geoscience and Remote Sensing Letters*, vol.11, no.4, pp.788–792, 2014.

[6] C. Poullis and S. You, Delineation and geometric modeling of road networks, *ISPRS Journal of Photogrammetry and Remote Sensing*, vol. 65, no. 2, pp. 165–181, 2010.

[7] W. Sun and D. W. Messinger, Knowledge-based automated road network extraction system using multispectral images, *Optical Engineering*, vol.52, no.4, pp.047203-1–047203-14, 2013.

[8] J. Hu, A. Razdan, J. C. Femiani, M. Cui, and P. Wonka, Road network extraction and intersection detection from aerial images by tracking road footprints, *IEEE Transactions on Geoscience and Remote Sensing*,vol.45, no.12, pp.4144–4157, 2007.

[9] M. Fauvel, J. A. Benediktsson, J. Chanussot, and J. R. Sveinsson, Spectral and spatial classification of hyperspectral data using SVMs and morphological profiles, *IEEE Transactions on Geoscience and Remote Sensing*, vol.46, no.11, pp.3804–3814, 2008.

[10] Y. T. Zhou, V. Venkateswar, and R. Chellapa, Edge detection and linear feature extraction using a 2-D random field model, *IEEE Transactions on Pattern Analysis and Machine Intelligence*, vol.11, no.1, pp.84–95, 1989.

[11] I. Laptev, H. Mayer, T. Lindeberg, W. Eckstein, C. Steger, and A. Baumgartner, Automatic extraction of roads from aerial images based on scale space and snakes, *Machine Vision and Applications* , vol.12, no.1, pp.23–31, 2000.

[12] H. Zhao , J. Kumagai, M. Nakagawa, and R. Shibasaki. Semi-automatic road extraction from high resolution satellite images. *Proceedings of ISPRS Photogrammetry and Computer Vision*, Graz, Austria2002.

[13] D. Geman and B. Jedynak, An active testing model for tracking roads in satellite images, *IEEE Transactions on Pattern Analysis and Machine Intelligence*, vol.18, no.1, pp.1–14, 1996.
[14] H. Blum, A transformation for extracting new parameter of shape, *Models for the Perception of Speech and Visual Form*, Cambridge, MA: MIT Press, pp.362–380, 1967.
[15] Y. Ge, D. Stelts, J. Wang, and D. Vining, Computing the centerline of the colon: a robust and efficient method based on 3D skeletons, *Journal of Computer Assisted Tomography*, vol.23, no.5, pp.786–794, 1999.
[16] G. Peyre, M. Pechaud, R. Keriven, and L. D. Cohen, Geodesic methods in computer vision and graphics, *Foundations and Trends in Computer Graphics and Vision* ,vol.5, no.3/4, pp.197–397, 2010.
[17] S. Kurugol, E. Bas, D. Erdogmus, J. G. Dy, G. C. Sharp, and D. H. Brooks, Centerline Extraction with Principal Curve Tracing to Improve 3D Level Set Esophagus Segmentation in CT Images, *The 33rd Annual International Conference of the IEEE Engineering in Medicine and Biology Society* , Boston, Massachusetts USA, PP.3403–3406, 2011.
[18] Z. Miao, W. Shi, H. Zhang, and X. Wang, Road centerline extraction from high-resolution imagery based on shape features and multivariate adaptive regression splines, *IEEE Geoscience and Remote Sensing Letters*, vol. 10, no.3, pp.583–587, 2013.
[19] M. B. Salah, A. Mitiche, I. B. Ayed. Multiregion image segmentation by parametric kernel graph cuts. *IEEE Transactions on Image Processing* , vol.20, no.2, pp.545–557, 2011.
[20] C. Panagiotakis, E. Kokinou, and A. Sarris, Curvilinear structure enhancement and detection in geophysical images, *IEEE Transactions on Geoscience and Remote Sensing*, vol.49, no.6, pp.2040–2048, 2011.
[21] J. H. Friedman, Multivariate Adaptive Regression Splines. *The Annals of Statistics*, vol.19, no.1, pp.1–67, 1991.
[22] http://cvlab.epfl.ch/data/delin/
[23] C. Wiedemann, C. Heipke, and H. Mayer, Empirical evaluation of automatically extracted road axes, *Proc. of the CVPR workshop on empirical evaluation methods in computer vision*, Los Alamitos, California, pp.172–187, 1998.